Hydrogen-Atom Tunneling of 2,5-Dichloro-3,6-dihydroxy-1,4-benzoquinone in a Low-Temperature Argon Matrix Studied by FTIR Spectroscopy

Nobuyuki Akai, Satoshi Kudoh, Masao Takayanagi, and Munetaka Nakata*

Graduate School of BASE (Bio-Applications and Systems Engineering), Tokyo University of Agriculture and Technology, Naka-cho, Koganei, Tokyo 184-8588, Japan

Received: May 7, 2002; In Final Form: August 22, 2002

Torsional isomerization around the two C−O bonds of 2,5-dichloro-3,6-dihydroxy-1,4-benzoquinone in a low-temperature argon matrix has been investigated by FTIR spectroscopy with an aid of the density functional theory calculations. The infrared spectrum of the most stable isomer, which has two intramolecular hydrogen bonds of C═O···H−O, was observed, while that of a less stable isomer, which has C═O···H−O and C−Cl···H−O hydrogen bonds, was observed as a transient species during UV−visible irradiation. Isomerization from the less stable isomer to the most stable one occurred immediately after the irradiation was stopped. This isomerization is ascribed to the effect of hydrogen-atom tunneling.

Introduction

Recently, tunneling chemical reactions at low temperature have become an interesting subject in interstellar chemistry.[1−3] It is known that the tunneling effect plays an important role in production of NH_3, CH_4, and formaldehyde from free atoms or small molecules or both in space, where the activation energies for these products are insufficient. One of the powerful techniques in laboratories to study the tunneling effect is microwave spectroscopy or laser spectroscopy with a supersonic expansion technique, which provides information on energy-level splittings due to this effect.[4,5]

On the other hand, low-temperature rare-gas matrix isolation prepares an extremely low-temperature and high-vacuum condition like space.[6,7] The hydrogen-atom tunneling in tropolone,[8−10] malonaldehyde,[11] and 9-hydroxyphenalenone[12−15] has been studied by this technique combined with various spectroscopies.

The tunneling generally occurs on symmetrical double-minimum potential surfaces but not asymmetrical ones.[16,17] However, we have recently reported the possibility of a matrix-induced tunneling in hydroquinone (HYQ) in low-temperature rare-gas matrixes.[18] HYQ has an asymmetrical double-minimum potential surface between cis and trans isomers. Although hydrogen-atom tunneling does not occur in the gas phase,[19] the cis isomer produced by UV irradiation in low-temperature rare-gas matrixes changed immediately into the more stable isomer, trans, in dark after the irradiation was stopped. Then, we concluded that hydrogen-atom tunneling occurred on a quasi-symmetrical double-minimum potential perturbed by an interaction between HYQ and matrix media, where thermal isomerization equilibrium was impossible because of the high torsional barrier, 10.8 kJ mol^{-1}.

In the present study, we have investigated the hydrogen-atom tunneling of 2,5-dichloro-3,6-dihydroxy-1,4-benzoquinone (chloranilic acid, called CA hereafter) in a low-temperature argon matrix by FTIR spectroscopy. CA has three stable isomers shown in Figure 1, where isomer I has two C═O···H−O, isomer II has C═O···H−O and C−Cl···H−O, and isomer III has two C−Cl···H−O hydrogen bonds. Two kinds of hydrogen-atom transfer can occur in this molecule; one is torsional isomerization among these isomers on the asymmetrical potential surface, and the other is the intramolecular double hydrogen-atom transfer in isomer I on the symmetrical potential surface, as shown in Figure 2. To our knowledge, no vibrational spectroscopic studies on any isomers have yet been published. One of the purposes of the present study is to analyze the isomerization of CA in low-temperature argon matrixes by FTIR spectroscopy and compare the hydrogen-atom tunneling with that of HYQ. "Intermolecular" double hydrogen-atom transfer has been studied in molecules such as 7-azaindol dimer [20] and carboxylic

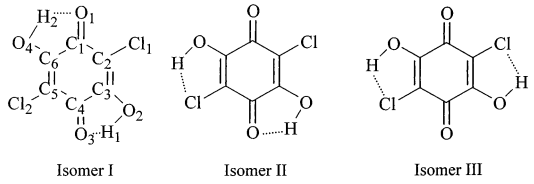

Figure 1. Three stable rotational isomers of 2,5-dichloro-3,6-dihydroxy-1,4-benzoquinone. Numbering of atoms is given in isomer I.

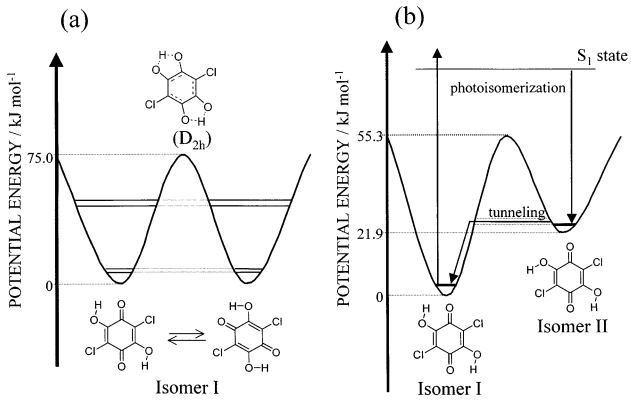

Figure 2. Schematic potential energy surfaces: (a) a symmetrical double-minimum potential surface of isomer I; (b) an asymmetrical double-minimum potential surface between isomers I and II. The energy levels are calculated by the DFT/B3LYP/6-31++G**.

* To whom correspondence should be addressed. E-mail: necom@cc.tuat.ac.jp. Tel: +81-42-388-7349. Fax: +81-42-388-7349.

10.1021/jp021136h CCC: $22.00
Published on Web 10/29/2002

acid dimer;[21] however, fewer papers on "intramolecular" double hydrogen-atom transfer have been published.

Experimental Methods and Calculations

Because the vapor pressure of CA, purchased form Tokyo Chemical Industry Co. Ltd., was too low to transfer the vapor sufficiently into a glass cylinder, a small amount of the solid was placed in a stainless steel pipe nozzle with a heating system, on which pure argon gas (Nippon Sanso, 99.9999% purity) was flowed. The sample was heated to about 380 K, and the flow rate of rare gas was adjusted to obtain sufficient isolation. The mixed gas was expanded through a stainless steel pipe and deposited in a vacuum chamber on a CsI plate cooled by a closed-cycle helium refrigerator (CTI Cryogenics, model M-22) at about 16 K. UV and visible radiation from a superhigh-pressure mercury lamp was used to increase the population of the less stable isomer. A water filter was used to remove thermal reactions, and Y-45, L-42, UV-32, and UV-30 cutoff filters (HOYA) were used to select irradiation wavelength. Infrared spectra of the matrix samples were measured with an FTIR spectrophotometer (JEOL, model JIR-7000). The spectral resolution was 0.5 cm^{-1}, and the accumulation number was 64. Other experimental details were reported elsewhere.[22,23]

Density functional theory (DFT) calculations were performed using the Gaussian 98 program[24] with the 6-31++G** basis set. The hybrid density functional,[25] in combination with the Lee−Yang−Parr correlation functional (B3LYP),[26] was used to optimize the geometrical structures for the ground state and the lowest electronically excited triplet state. Open shell wave functions were used for the triplet state.

Results and Discussion

Optimized Geometries. The optimized geometries and the vibrational wavenumbers for the three stable isomers were calculated at the DFT/B3LYP/6-31++G** level. All of the geometries were found to be planar, where isomers I and III have C_{2h} symmetry. Isomer I, which has two C═O···H−O hydrogen bonds, is the most stable isomer. The relative energies of isomers I, II, and III were calculated to be 0, 21.9, and 40.3 kJ mol^{-1}, respectively. The order of the stability may be explained in terms of the strength of the hydrogen bonding; C═O···H−O is stronger than C−Cl···H−O because the electronegativity of oxygen atom is higher than that of chlorine atom. The calculated geometrical parameters are summarized in Table 1. The C═O···H−O distance of isomer I, 1.979 Å, is about 0.6 Å shorter than the sum of the van der Waals radii of oxygen and hydrogen atoms, 2.60 Å. Similar shortenings are found in isomers II and III, for which the C−Cl···H−O distance of Isomer III, 2.469 Å, is shorter than the sum, 3.0 Å, and C═O···H−O, 2.014 Å, and C−Cl···H−O, 2.479 Å, distances of isomer II are shorter than the corresponding sums. Torsional isomerization barriers between isomers I and II and between isomers II and III are calculated to be 55.3 and 71.8 kJ mol^{-1}, respectively. These barrier heights are much higher than that for HYQ, 10.8 kJ mol^{-1}, reported in our recent paper.[18] The barrier height for the double hydrogen-atom transfer in Isomer I is also calculated to be 75.0 kJ mol^{-1}. A schematic energy diagram is shown in Figure 2.

Analysis of Infrared Spectrum. The spectrum of argon-matrix isolated species measured with an FTIR spectrophotometer is shown in Figure 3a. Most of the bands observed in the region higher than 800 cm^{-1} showed splittings. One possibility for these splittings is the matrix-site effect. If this were the case, these splittings may disappear by an annealing at about 28 K in argon matrixes. However, only a small change in their relative intensities was found. This observation suggested that the origin of the splittings in our observed spectrum was not the site effect. An attempt to interpret the splittings by Fermi resonance or combination of the fundamental bands could explain only a few of them. Then, we assumed that these splittings were caused by the intramolecular double hydrogen-atom tunneling in isomer

TABLE 1: Optimized Geometrical Parameters of Three Stable Isomers of 2,5-Dichloro-3,6-dihydroxy-1,4-benzoquinone Obtained at the DFT/B3LYP/6-31++G Level**

Bond Length (Å)

parameter[a]	isomer I	isomer II	isomer III
C_1-C_2	1.455	1.474	1.471
C_2-C_3	1.359	1.356	1.357
C_3-C_4	1.521	1.508	1.514
C_4-C_5	1.455	1.455	1.471
C_5-C_6	1.359	1.359	1.357
C_6-C_1	1.521	1.524	1.514
O_1-C_1	1.228	1.216	1.217
O_2-C_3	1.324	1.331	1.333
O_3-C_4	1.228	1.228	1.217
O_4-C_6	1.324	1.329	1.333
Cl_1-C_2	1.729	1.728	1.743
Cl_2-C_5	1.729	1.743	1.743
H_1-O_2	0.983	0.981	0.973
H_1-O_3	1.979	2.014	
H_2-O_4	0.983	0.973	0.973
H_2-Cl_2		2.479	2.469

Bonding Angle (deg)

parameter[a]	isomer I	isomer II	isomer III
$C_1-C_2-C_3$	118.7	120.5	122.4
$C_2-C_3-C_4$	122.4	122.0	121.3
$C_3-C_4-C_5$	118.8	118.0	116.2
$C_4-C_5-C_6$	118.7	120.7	122.4
$C_5-C_6-C_1$	122.4	121.7	121.3
$C_6-C_1-C_2$	118.8	117.1	116.2
$O_1-C_1-C_2$	125.4	123.9	123.6
$O_2-C_3-C_4$	113.8	114.1	113.4
$O_3-C_4-C_5$	125.4	125.0	123.6
$O_4-C_6-C_1$	113.8	113.3	113.4
$Cl_1-C_2-C_3$	122.5	121.8	120.0
$Cl_2-C_5-C_6$	122.5	120.7	120.0
$H_1-O_2-C_3$	106.2	106.5	109.5
$H_2-O_4-C_6$	106.2	109.7	109.5

[a] Numbering of atoms is given in Figure 1.

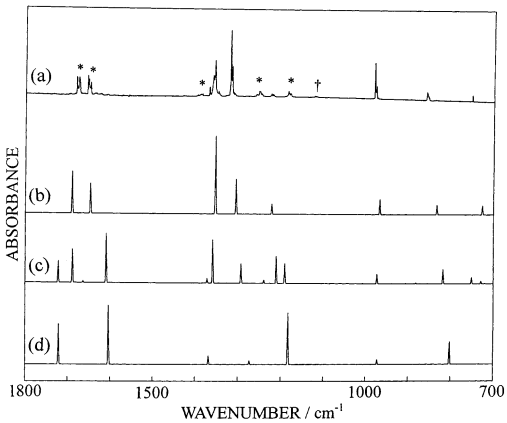

Figure 3. Infrared spectra of 2,5-dichloro-3,6-dihydroxy-1,4-benzoquinone: (a) observed matrix spectrum. Bands marked with * and † represent infrared inactive modes and combination modes, respectively. Spectra b−d are calculated spectral patterns for isomers I, II, and III, respectively, obtained at the DFT/B3LYP/6-31++G** level, where a scaling factor of 0.98 is used.

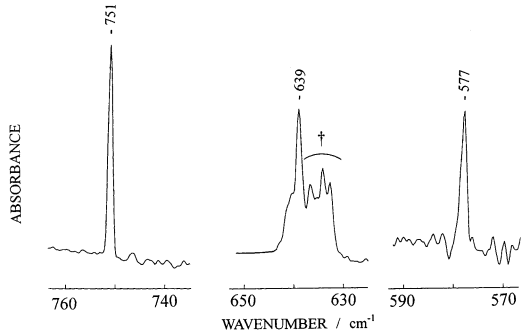

Figure 4. Infrared bands of a_u modes of 2,5-dichloro-3,6-dihydroxy-1,4-benzoquinone. Bands marked with † represent a combination mode.

I, as well as the parent molecule of CA, 2,5-dihydroxy-1,4-benzoquinone.[27,28]

The observed spectrum is compared with the calculated spectral patterns of the three isomers in Figure 3. All of the calculated wavenumbers are scaled by a factor of 0.98.[29] It is found that the calculated spectral pattern of isomer I reproduces the observed spectrum more satisfactorily than those of the other isomers, especially in the C═O and C═C stretching regions. However, some bands marked with * remain unassigned to isomer I. These excess bands appear near the wavenumbers of infrared inactive modes of isomer I. The reason the infrared inactive modes appear in our infrared spectrum can be explained by the hydrogen-atom tunneling as follows.

Because CA has C_{2h} symmetry, the vibrational modes can be classified into four groups, that is, a_g, b_g, a_u, and b_u. The a_g and b_g modes are infrared inactive, while a_u and b_u are infrared active. The a_g and b_u modes are in-plane vibrational modes, which are coupled with the hydrogen-atom tunneling motion. Therefore, the infrared inactive a_g modes appear in the region higher than 800 cm^{-1} with splittings due to the tunneling effect, as well as the infrared active b_u modes. On the other hand, the b_g and a_u modes are out-of-plane vibrational modes, which are not coupled with the tunneling motion. Then, the infrared active a_u modes appearing at 751, 639, and 577 cm^{-1} show no splitting due to the tunneling as shown in Figure 4, where the bands marked with †, appearing around the 639 cm^{-1} band, are assignable to a combination mode. No bands assignable to the infrared inactive out-of-plane b_g modes appear in our infrared spectrum.

The observed and calculated wavenumbers of isomer I are summarized with their intensities and symmetries of the vibrational modes in Table 2. No bands of the other isomers were observed in our matrix spectrum. This result is consistent with the population ratio of isomers estimated from the calculated energy differences among the isomers using the Boltzmann distribution law; the populations of less stable isomers II and III are estimated to be less than 1% of isomer I at the nozzle temperature, 380 K.

Spectrum of Transient Species. No change was observed in a difference spectrum between those measured before and after UV−visible irradiation. Contrary to this observation, new bands appeared in a difference spectrum between those measured during and after the UV−visible irradiation through a UV-30 cutoff filter, as shown in Figure 5a; the increasing and decreasing bands are due to a photoproduced transient species and the reactant, isomer I, respectively. It was found that the absorbance of isomer I decreased by about 11% during the UV-30 irradiation. These bands of the transient species disappeared completely when the irradiation was stopped. A similar spectral change was observed using a Y-45 cutoff filter, the irradiation

TABLE 2: Observed and Calculated Vibrational Wavenumbers (in cm^{-1}) and Relative Intensities of Isomer I

obsd		calcd		
ν	int	ν^a	IR int	symmetry
3371	12.9	3492	40.2	b_u
3366[b]	12.8	3486	0	a_g
1680	27.7	1697	0	a_g
1675[b]	25.0	1690	53.6	b_u
1655[b]	28.1	1655	0	a_g
1648[b]	20.3	1647	38.6	b_u
1368	12.6	1377	0	a_g
1356[b]	52.8	1353	100	b_u
1319[b]	100	1305	45.0	b_u
1253[b]	7.2	1253	0	a_g
1224[b]	3.8	1222	13.0	b_u
1185[b]	8.0	1214	0	a_g
1122[b,c]	1.6			
980[b]	56.4	967	19.5	b_u
		893	0	a_g
858[b]	12.7	833	12.3	b_u
		763	0	a_g
751	9.1	726	11.5	a_u
		701	0	b_g
639	13.8	688	13.2	a_u
632[b,c]	6.4			
		680	0	b_g
577	17.9	573	3.6	a_u

[a] A scaling factor of 0.98 is used. [b] Splitting bands. [c] Assigned to combination modes.

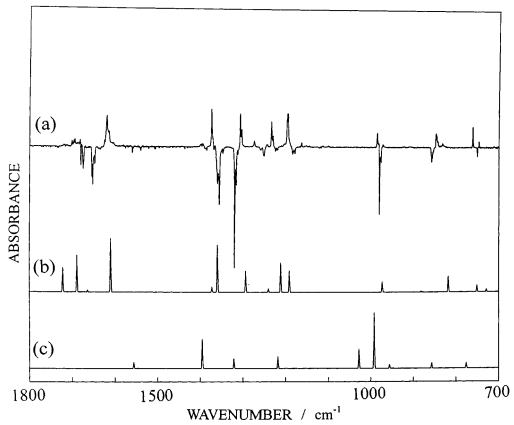

Figure 5. Infrared spectrum of transient species of 2,5-dichloro-3,6-dihydroxy-1,4-benzoquinone: (a) difference spectrum between those measured during and after UV irradiation through a UV-30 cutoff filter. Increasing bands are due to a transient species, while decreasing bands correspond to those of reactant, isomer I. Spectra b and c are calculated spectral patterns for isomer II and the lowest electronically excited triplet state of isomer I, respectively, obtained at the DFT/B3LYP/6-31++G** level, where a scaling factor of 0.98 is used.

wavelength of which nearly corresponds to the electronic transition energy from S_0 to S_1 states of CA (λ_{max} = 452 nm in methanol solution).

The spectral change in the OH stretching region is expanded in Figure 6a, where two bands of the transient species appeared at 3518 and 3395 cm^{-1}. The wavenumbers of these bands are lower than that of the free OH stretching of HYQ, 3600 cm^{-1}.[18] The 3518 and 3395 cm^{-1} bands are assignable to the OH stretching in C−Cl···H−O and C═O···H−O hydrogen bondings, respectively. This assignment suggests that the transient species can be identified as isomer II, which has the C−Cl···H−O and C═O···H−O hydrogen bonds. The calculated spectral pattern of isomer II is compared with the observed spectrum of the transient species in Figures 5 and 6. The intensities of the carbonyl stretching bands around 1700 cm^{-1} in the observed

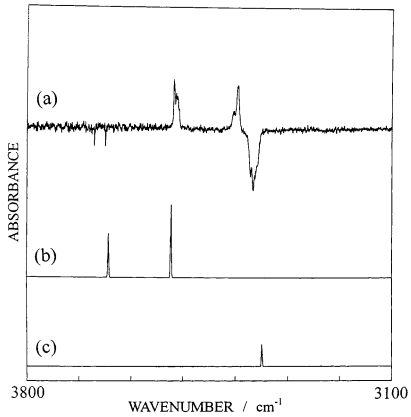

Figure 6. O−H stretching region of transient species of 2,5-dichloro-3,6-dihydroxy-1,4-benzoquinone: (a) difference spectrum between those measured during and after UV irradiation through a UV-30 cutoff filter. Increasing bands are due to a transient species, while decreasing band corresponds to that of reactant, isomer I. Spectra b and c are calculated spectral patterns for isomer II and the lowest electronically excited triplet state of isomer I, respectively, obtained at the DFT/B3LYP/6-31++G** level, where a scaling factor of 0.98 is used.

TABLE 3: Observed and Calculated Vibrational Wavenumbers (in cm^{-1}) and Relative Intensities of Isomer II

obsd		calcd	
ν	int	ν^a	IR int
3518[b]	32.8	3643	22.8
3395[b]	36.4	3522	38.1
1702[b]	12.6	1722	44.2
1682	15.4	1689	68.0
		1664	3.6
1620	83.3	1610	100
1395	3.2	1372	9.5
1374	100	1359	88.0
1307[b]	87.9	1293	39.8
1274	13.6	1240	6.7
1234[b]	68.0	1211	55.2
1196[b]	88.3	1191	40.2
1164[c]	10.9		
986	41.0	973	19.1
		882	1.8
848[b]	42.5	818	29.5
832[c]	13.2		
761	62.0	751	12.5
747	20.9	729	4.9
		667	7.0
		652	16.7
583	89.2	571	21.8

[a] A scaling factor of 0.98 is used. [b] Splitting bands. [c] Assigned to combination modes.

spectrum seem to be slightly weaker than those of the corresponding calculated values, because they split and overlap with the decreasing bands of isomer I. The observed and calculated wavenumbers of isomer II are summarized in Table 3 with their relative intensities. The bands appearing at 1164 and 832 cm^{-1} are assumed to be due to combination modes.

A question arises here why the bands of isomer II disappeared immediately after the irradiation was stopped. Because thermodynamical isomerization hardly occurs in low-temperature conditions if its torsional isomerization barrier is higher than 5 kJ mol^{-1},[30−32] the less stable isomer produced by the irradiation should have survived in the matrix and exhibited its spectrum.

The transient species produced from isomer I during the irradiations may be assigned to the lowest electronically excited triplet state of CA. In fact, infrared spectra of triplet states are measurable with a conventional FTIR spectrophotometer, for example, that of naphthalene.[33] However, the result of our calculation for the T_1 state of isomer I is inconsistent with the observed spectrum of the transient species. Especially, the transient species has two bands in the OH stretching region between 3800 and 3100 cm^{-1}, but the calculated results show only one band in this region. Then, the triplet state is removed from the candidates of the transient species.

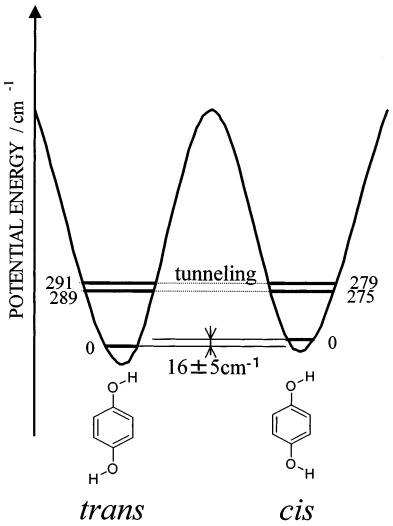

Figure 7. Schematic potential energy surface of hydroquinone. The vibration levels are calculated by the DFT/B3LYP/6-31++G**. The enthalpy difference between the isomers is determined by a xenon-matrix experiment.[18]

Many studies on infrared-induced rotational isomerization by the matrix isolation techniques have been published.[34−38] Some of them suggest that the isomerization might be caused by tunneling effect, because the isomerization occurred not only by infrared radiation but also in dark in low-temperature conditions.[36−38] As for CA, isomer II disappeared within at most a few seconds after the irradiation was stopped. Then, infrared-induced isomerization is to be excluded, but the hydrogen-atom tunneling is permissible in dark.

Comparison of Tunneling Effects in CA and HYQ. For HYQ, the torsional barrier height was estimated to be 10.8 kJ mol^{-1}. This value is too high for the cis/trans isomerization to occur at the matrix temperature in thermal equilibrium.[30] Then, the disappearance of the cis bands in dark was explained by the hydrogen-atom tunneling effect.[18] In the case of CA, the barrier height for isomerization from isomer II to I is 33.4 kJ mol^{-1}, which is 3 times as high as that of HYQ. Therefore, the thermodynamical isomerization at the matrix temperature is impossible, even if the barrier height is somewhat decreased in the matrix. Then, we conclude that the relaxation from isomer II to I in dark is caused by tunneling as in HYQ.

The isomerization mechanism for HYQ caused by matrix-induced hydrogen-atom tunneling[18] is shown in Figure 7, where the potential surface perturbed by a matrix medium is quasi-symmetrical double-minimum potential. The energy difference between the isomers in the matrix, 16 ± 5 cm^{-1}, is one-third of the calculated value, 48 cm^{-1}. The vibrational energies of the torsional motions associated with the isomerization were calculated to be 279 and 275 cm^{-1} for cis and 291 and 289 cm^{-1} for trans. Because the zero-point vibrational energy level of cis is 16 ± 5 cm^{-1} higher than that of trans, the torsional motions of cis are 295 ± 5 and 291 ± 5 cm^{-1} scaled from the zero-point energy level of trans. These values correspond to those of the torsional motions of trans. These findings suggest the hydrogen-atom tunneling pathway in the matrix.

The calculated potential surface and tentative isomerization pathway for CA are drawn schematically in Figure 2b. The energy difference between isomers I and II is calculated to be 21.9 kJ mol^{-1}, which is much higher than that between cis and trans of HYQ. The energy difference is so large that the details on the resonance of the energy levels for the two isomers are unknown. However, we cannot explain the isomerization without the hydrogen-atom tunneling, although the barrier height seems to be too high. An accurate analysis for the tunneling mechanism is left for a future study.

Summary

2,5-Dichloro-3,6-dihydroxy-1,4-benzoquinone in a low-temperature argon matrix has been studied by FTIR spectroscopy with an aid of the DFT calculations. The observed infrared spectrum is assigned to isomer I, which has two C═O···H−O hydrogen bonds. The band splittings and the appearance of the infrared inactive modes can be explained by the intramolecular double hydrogen-atom tunneling on a symmetrical double-minimum potential surface. The infrared spectrum of a less stable isomer II, which has C═O···H−O and C−Cl···H−O bonds, was observed during the UV−visible irradiation as a transient species. Isomer II returns to the most stable isomer I in dark at 16 K. This isomerization can be explained by the hydrogen-atom tunneling on an asymmetrical potential surface.

Acknowledgment. The authors thank Professor Kozo Kuchitsu (Faculty of Science, Josai University) for his helpful discussion.

References and Notes

(1) Hiraoka, K.; Ohashi, N.; Kihara, Y.; Yamamoto, K.; Sato, T.; Yamashita, A. *Chem. Phys. Lett.* **1994**, *229*, 408.

(2) Hiraoka, K.; Takayama, T.; Euchi, A.; Handa, H.; Sato, T. *Astrophys. J.* **2000**, *532*, 1029.

(3) Hiraoka, K.; Sato, T.; Takayama, T. *Science* **2001**, *292*, 869.

(4) Rowe, W. F., Jr.; Duerst, R. W.; Wilson, E. B. *J. Am. Chem. Soc.* **1976**, *98*, 4021.

(5) Redington, R. L.; Chen, Y.; Scherer, G. J.; Field, R. W. *J. Chem. Phys.* **1988**, *88*, 627.

(6) Hallou, A.; Schriver-Mazzuoli, L.; Schriver, A.; Chaquin, P. *Chem. Phys.* **1998**, *237*, 251.

(7) Komaguchi, K.; Kumada, T.; Aratono, Y.; Miyazaki, T. *Chem. Phys. Lett.* **1997**, *268*, 493.

(8) Redington, R. L.; Redington, T. E. *J. Mol. Spectrosc.* **1979**, *78*, 229.

(9) Redington, R. L. *J. Chem. Phys.* **1990**, *92*, 6447.

(10) Redington, R. L.; Redington, T. E.; Montgomery, J. M. *J. Chem. Phys.* **2000**, *113*, 2304.

(11) Firth, D. W.; Barbara, P. F.; Trommsdorf, H. P. *Chem. Phys.* **1989**, *136*, 349.

(12) Rossetti, R.; Haddon, R. C.; Brus, L. E. *J. Am. Chem. Soc.* **1980**, *102*, 6913.

(13) Bondybey, V. E.; Haddon, R. C.; English, J. H. *J. Chem. Phys.* **1984**, *80*, 5432.

(14) Bondybey, V. E.; Haddon, R. C.; Rentzepis, P. M. *J. Am. Chem. Soc.* **1984**, *106*, 5969.

(15) Barbara, P. F.; Walsh, P. K.; Brus, L. E. *J. Phys. Chem.* **1989**, *93*, 29.

(16) Frei, H.; Pimentel, G. C. *J. Phys. Chem.* **1981**, *85*, 3355.

(17) Szczepanski, J.; Ekern, S.; Vala, M. *J. Phys. Chem.* **1995**, *99*, 8002.

(18) Akai, N.; Kudoh, S.; Takayanagi, M.; Nakata, M. *Chem. Phys. Lett.* **2002**, *356*, 133.

(19) Caminati, W.; Melandri, S.; Favero, L. B. *J. Chem. Phys.* **1994**, *100*, 8569.

(20) Catalan, J.; Kasha, M. *J. Phys. Chem. A* **2000**, *104*, 10812.

(21) Meier, B. H.; Graf, F.; Emst, R. R. *J. Chem. Phys.* **1982**, *76*, 767.

(22) Nakata, M.; Kudoh, S.; Takayanagi, M.; Ishibashi, T.; Kato, C. *J. Phys. Chem. A* **2000**, *104*, 11304.

(23) Kudoh, S.; Takayanagi, M.; Nakata, M. *J. Photochem. Photobiol., A* **1999**, *123*, 25.

(24) Frisch, M. J.; Trucks, G. W.; Schlegel, H. B.; Scuseria, G. E.; Robb, M. A.; Cheeseman, J. R.; Zakrzewski, V. G.; Montgomery, J. A., Jr.; Stratmann, R. E.; Burant, J. C.; Dapprich, S.; Millam, J. M.; Daniels, A. D.; Kudin, K. N.; Strain, M. C.; Farkas, O.; Tomasi, J.; Barone, V.; Cossi, M.; Cammi, R.; Mennucci, B.; Pomelli, C.; Adamo, C.; Clifford, S.; Ochterski, J.; Petersson, G. A.; Ayala, P. Y.; Cui, Q.; Morokuma, K.; Malick, D. K.; Rabuck, A. D.; Raghavachari, K.; Foresman, J. B.; Cioslowski, J.; Ortiz, J. V.; Stefanov, B. B.; Liu, G.; Liashenko, A.; Piskorz, P.; Komaromi, I.; Gomperts, R.; Martin, R. L.; Fox, D. J.; Keith, T.; Al-Laham, M. A.; Peng, C. Y.; Nanayakkara, A.; Gonzalez, C.; Challacombe, M.; Gill, P. M. W.; Johnson, B. G.; Chen, W.; Wong, M. W.; Andres, J. L.; Head-Gordon, M.; Replogle, E. S.; Pople, J. A. *Gaussian 98*, revision A.6; Gaussian, Inc.: Pittsburgh, PA, 1998.

(25) Becke, A. D. *J. Chem. Phys.* **1993**, *98*, 5648.

(26) Lee, C.; Yang, W.; Parr, R. G. *Phys. Rev. B* **1988**, *37*, 785.

(27) Graf, F. *Chem. Phys. Lett.* **1979**, *62*, 291.

(28) Redington, R. L.; Redington, T. E.; Rajaram, B.; Field, R. W. *J. Chem. Phys.* **1992**, *97*, 1624.

(29) Akai, N.; Takayanagi, M.; Nakata, M. *Jpn. Chem. Program Exch. J.* **2001**, *13*, 97.

(30) Barnes, A. J. In *Matrix Isolation Spectroscopy*; Barnes, A. J., Orville-Thomas, W. J., Müller, A., Gaufrés, R., Eds.; Reidel: Dordrecht, Netherlands, 1981; p 531.

(31) Nagashima, N.; Kudoh, S.; Takayanagi, M.; Nakata, M. *J. Phys. Chem. A* **2001**, *105*, 10832.

(32) Kudoh, S.; Uechi, T.; Takayanagi, M.; Nakata, M.; Tanaka, N.; Shibuya, K. *J. Mol. Struct.* **2000**, *524*, 251.

(33) Kudoh, S.; Takayanagi, M.; Nakata, M. *J. Mol. Struct.* **1999**, *475*, 253.

(34) Hall, R. T.; Pimentel, G. C. *J. Chem. Phys.* **1963**, *38*, 1889.

(35) Knudsen, A. K.; Pimentel, G. C. *J. Chem. Phys.* **1983**, *78*, 6780.

(36) Kudoh, S.; Takayanagi, M.; Nakata, M.; Ishibashi, T.; Tasumi, M. *J. Mol. Struct.* **1999**, *479*, 41.

(37) Aspiala, A.; Lotta, T.; Murto, J.; Räsänen, M. *J. Chem. Phys.* **1983**, *79*, 4183.

(38) Räsänen, M.; Schwartz, G. P.; Bondybey, V. E. *J. Chem. Phys.* **1986**, *84*, 59.